Journal of ELECTRONIC MATERIALS, Vol. 47, No. 3, 2018
https://doi.org/10.1007/s11664-017-6017-4

Stable Ferroelectric Behavior of Nb-Modified $Bi_{0.5}K_{0.5}TiO_3$-$Bi(Mg_{0.5}Ti_{0.5})O_3$ Lead-Free Relaxor Ferroelectric Ceramics

ARIF ZAMAN,[1,2] RIZWAN AHMED MALIK,[1] ADNAN MAQBOOL,[1,3] ALI HUSSAIN,[1,4] TANVEER AHMED,[2] TAE KWON SONG,[1] WON-JEONG KIM,[5] and MYONG-HO KIM[1,6]

1.—School of Advanced Materials Engineering, Changwon National University, Gyeongnam 641-773, Republic of Korea. 2.—Department of Physics, Abdul Wali Khan University, Mardan, KPK, Pakistan. 3.—Department of Metallurgical and Materials Engineering, University of Engineering and Technology, Lahore, Pakistan. 4.—Department of Materials Science and Engineering, Institute of Space Technology, Islamabad, Pakistan. 5.—Department of Physics, Changwon National University, Gyeongnam 641-773, Republic of Korea. 6.—e-mail: mhkim@changwon.ac.kr

Crystal structure, dielectric, ferroelectric, piezoelectric, and electric field-induced strain properties of lead-free Nb-modified $0.96Bi_{0.5}K_{0.5}TiO_3$-$0.04Bi(Mg_{0.5}Ti_{0.5})O_3$ (BKT-BMT) piezoelectric ceramics were investigated. Crystal structure analysis showed a gradual phase transition from tetragonal to pseudocubic phase with increasing Nb content. The optimal piezoelectric property of small-signal d_{33} was enhanced up to $\sim$ 68 pC/N with a lower coercive field (E_c) of $\sim$ 22 kV/cm and an improved remnant polarization (P_r) of $\sim$ 13 μC/cm^2 for x = 0.020. A relaxor-like behavior with a frequency-dependent Curie temperature T_m was observed, and a high T_m around 320°C was obtained in the investigated system. This study suggests that the ferroelectric properties of BKT-BMT was significantly improved by means of Nb substitution. The possible shift of depolarization temperature T_d toward high temperature T_m may have triggered the spontaneous relaxor to ferroelectric phase transition with long-range ferroelectric order without any traces of a nonergodic relaxor state in contradiction with $Bi_{0.5}Na_{0.5}TiO_3$-based systems. The possible enhancement in ferroelectric and piezoelectric properties near the critical composition x = 0.020 may be attributed to the increased anharmonicity of lattice vibrations which may facilitate the observed phase transition from a low-symmetry tetragonal to a high-symmetry cubic phase with a decrease in the lattice anisotropy of an undoped sample. This highly flexible (at a unit cell level) narrow compositional range triggers the enhancement of d_{33} and P_r values.

Key words: Lead-free, piezoelectricity, ferroelectricity, phase transitions, electrical properties

INTRODUCTION

Currently, polycrystalline $Pb(Zr,Ti)O_3$ (PZT) and $Pb(Mg,Nb)O_3$-$PbTiO_3$ (PMN-PT) lead-based ceramic materials with excellent electromechanical response in a wide working temperature range ($\sim$ 386°C) are dominant in the global electronic market for various applications such as sensors and actuators. However, due to environmental concerns regarding lead-based materials, attention has been diverted towards environmentally benign materials to replace toxic Pb-based ceramics.[1,2] In this scenario, several Bi-based lead-free piezoelectric materials like $Bi_{0.5}Na_{0.5}TiO_3$ (BNT), $Bi_{0.5}K_{0.5}TiO_3$ (BKT), and $BiFeO_3$ have become the focus of intense research

(Received August 17, 2017; accepted December 8, 2017; published online December 20, 2017)
Arif Zaman, Rizwan Ahmed Malik, and Adnan Maqbool have contributed equally to this work.

due to the lone-pair 6s electronic configuration similar to Pb-based systems. However, main drawbacks of BNT-based materials are difficulty in poling, high conductivity, and high coercive field (E_c).[3] Furthermore, pure $BiFeO_3$ is difficult to synthesize due to its narrow temperature range of phase stabilization and formation of impurity phases.[4]

Another Bi-based perovskite material $Bi_{0.5}K_{0.5}TiO_3$ (BKT) with a high Curie temperature (T_C = 380°C) comparable to lead-based materials could be a promising candidate for practical applications.[5] However, volatilization of Bi_2O_3 and K_2CO_3 at high temperature hinders the highly dense pure BKT ceramics, which results in low electrical properties. Thus, some modifications should be made to obtain high-density samples and further improve the electrical properties. Various BKT-based solid solutions previously synthesized with other perovskites, such as BKT-$BaTiO_3$,[6] BKT-BNT,[7] BKT-$BiFeO_3$,[8] BKT-$K_{0.5}Na_{0.5}NbO_3$,[9] BKT-$Bi_{0.5}K_{0.5}ZrO_3$,[10] BKT-$Bi(Mg_{0.5}Ti_{0.5})O_3$,[11] BKT-$Bi(Mg_{2//3}Nb_{1/3})O_3$,[12] BKT-$BaNb_2O_3$,[13] and BKT-$BiFeO_3$-$NdFeO_3$-$Nd_{2/3}TiO_3$,[14] have been made to enhance the piezoelectric properties. Among these solid solutions, the binary BNT-BKT solid solution having a rhombohedral-tetragonal morphotropic phase boundary was one of the most widely studied systems due to its optimized piezoelectric performance with a piezoelectric charge coefficient ~ 150 pC/N.[7,15] Nevertheless, piezoelectric properties of BNT-BKT systems are significantly degraded around ~ 130°C, the so-called depolarization temperature (T_d), which limits the maximum operating temperature to < 130°C.

Hu et al.[16] studied the enhanced relaxor behavior of BKT with the addition of $Bi(Mg_{0.5}Ti_{0.5})O_3$ (BMT). They observed weakened depolarization temperature anomalies at T_d with the addition of BMT and observed a much higher T_d value (~ 187°C) compared to a T_d of ~ 136°C for the BNT-BMT system. For practical purposes, the higher T_d values are essential for a broader working temperature range.[17] Previously, Zeb et al. studied the binary composition (1-x) of BKT-x $Bi(Mg_{0.5}Ti_{0.5})O_3$ and observed enhance electromechanical properties at the mixed-phase region of the morphotropic phase boundary for compositions ($0.04 \le x \le 0.06$).[18]

In the present work, for the sake of improving ferroelectric performance in BKT-based materials, the above system [(1-x)BKT-xBi $(Mg_{0.5}Ti_{0.5})O_3$ with x = 0.04] was chosen as a base composition and the effect of Nb content on their properties was studied. Lead-free Nb-doped BKT-BMT solid solutions with a high Curie temperature were synthesized by a conventional mixed-oxide route and the effects of Nb doping on structural and electromechanical properties were studied in detail. The processing conditions such as calcination, sintering temperature, and soaking time were optimized. The effect of Nb modification on crystal structure, dielectric, ferroelectric, piezoelectric, and electric-field-induced strain measurements were studied. Furthermore, the underlying mechanism of improved ferroelectric properties and their stability are also discussed.

EXPERIMENTAL PROCEDURE

Piezoelectric ceramics with composition $0.96Bi_{0.5}K_{0.5}Ti_{1-x}Nb_xO_3$-$0.04Bi(Mg_{0.5}Ti_{0.5})O_3$ (x = 0–0.030) were synthesized by a conventional solid-state reaction technique. Commercially available reagent-grade oxide and carbonate powders of Bi_2O_3, TiO_2, K_2CO_3, MgO, MgO, and Nb_2O_5 (99.9% Sigma Aldrich Co. St. Louis, MO, USA) were used as starting materials. The hygroscopic K_2CO_3 powder was dried in an oven at 100°C for 24 h. For each composition, the starting materials were weighed according to the stoichiometric formula and powder mixtures were ball-milled for 24 h in ethanol with zirconia balls as the milling media. The slurries were subsequently dried and calcined at 850°C for 2 h. After calcinations, the mixtures were ball-milled for 24 h and dried. The dried powders were pulverized, mixed with an aqueous polyvinyl alcohol (PVA) solution as a binder for granulation, and passed through a 150-mesh sieve. Disk-shaped ceramic specimens with a diameter of 10 mm were then prepared by compacting the granulated powders at 98 MPa. The pressed discs were sintered at 1000°C, 1045°C, 1060°C, 1080°C, and 1100°C with soaking times of 3 h, 4 h, 5 h, and 8 h in covered alumina crucibles. To minimize the evaporation of the volatile elements Bi and Na, the disks were embedded in the powder of the same composition.

Silver paste was coated on both faces of the sintered samples and fired at 650°C for 0.5 h to form electrodes. The specimens used to measure the piezoelectric properties were poled in a silicone oil bath with a direct current (dc) field of 4 kV/mm for 15 min. All the electrical measurements were performed after aging for at least 24 h. The crystal structures were characterized using x-ray diffraction (XRD, X'pert MPD 3040, Philips, The Netherlands). Dielectric constant and loss of the ceramics were measured by an automatic acquisition system using an impedance analyzer (Agilent HP4292A, USA) in the temperature range of 25–400°C at different frequencies. The piezoelectric constant was measured using a Berlincourt d_{33} meter (IACAS, ZJ-6B). Polarization versus electric field (P–E) hysteresis loops were measured in silicon oil with the aid of a ferroelectric test system (Precision LC, Radian Technologies Inc., Albuquerque, NM, USA) at 20 Hz. Field-induced strain was measured with a contact type displacement sensor (Millitron; Model 140).

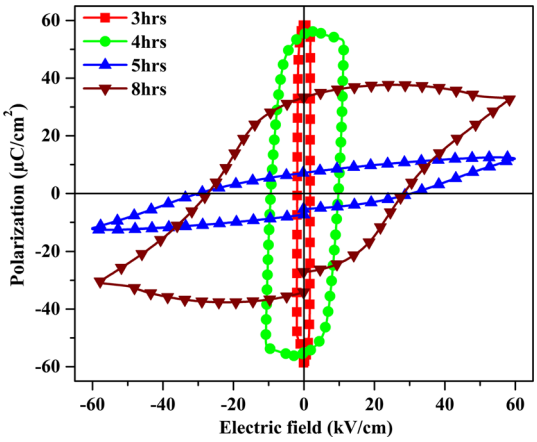

Fig. 1. Variation in polarization versus electric field response of unmodified BKT-BMT ceramics as a function of different soaking time at 1060°C.

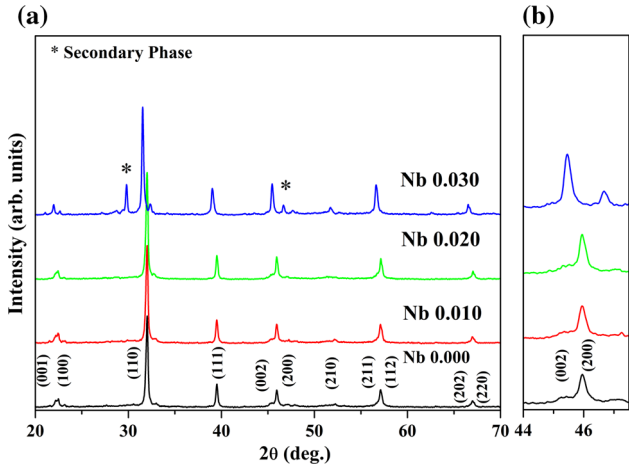

Fig. 2. X-ray diffraction patterns of Nb-modified BKT-BMT (x = 0.00–0.030) ceramics in the 2θ ranges of (a) 20°–70° and (b) 44°–47.5°.

RESULTS AND DISCUSSIONS

It is well-known that the sintering temperature and soaking time are of great importance to obtain high-density ceramics. For achieving optimized sintering conditions, the undoped BKT-BMT was sintered at different temperatures of 1000°C, 1045°C, 1060°C, 1080°C, and 1100°C with soaking times of 3 h, 4 h, 5 h, and 8 h. The base composition suffered from the high volatility of Bi and K at high temperatures of 1080°C and 1100°C.[11,17] For the sintering temperature $T <$ 1060°C, no dense ceramics were obtained. Therefore, the optimal sintering temperature for undoped BKT-BMT ceramics was found to be 1060°C with a 5-h soaking time. The effect of soaking time on the ferroelectric (FE) properties of undoped BKT-BMT is shown in Fig. 1. For a soaking time < 5 h, the absence of FE *P–E* loop of sintered samples (1060°C) showed the paraelectric phase of the material. With increasing soaking time, the FE property of the material was progressively improved. With further increase in soaking time up to 8 h, the sample showed leaky behavior which might be due to potentially increased volatility of Bi and K with increasing soaking time.[11,17] Hence, the optimal sintering temperature (1060°C) and soaking time (5 h) were selected for Nb-doped BKT-BMT ceramics.

Figure 2 shows the room-temperature XRD patterns of the as-sintered Nb-modified BKT-BMT ceramics. The specimens with Nb ≤ 0.020 appear to be a pure perovskite phase without any traces of secondary phase. This indicates that Nb has completely diffused into the BKT-BMT lattice forming a complete solid solution. In Fig. 2b, the split peaks at 46º indicate a tetragonal symmetry at room temperature for an unmodified sample, consistent with previous reports.[16,18]

For detailed phase structure evolution, the lattice parameters a and c, calculated from the XRD pattern peaks, and decreased tetragonality (c/a) of the BNKTN-BST ceramics are presented in Fig. 3a. The introduction of Nb content gradually reduces the tetragonality of BKT-BMT with increasing the flexibility of bonds between ions and their corresponding bond lengths with the possible increase in the anharmonicity of the crystal. This is supported by improved electromechanical properties (d_{33} value and ferroelectricity) in the compositional range from x = 0.00 to 0.020.[11–13,15,16] For $x \geq 0.020$, a compositional transition from tetragonal to pseudocubic symmetry was observed. At a further higher doping level of $x \geq 0.030$, a secondary phase was observed with degradation of FE properties. For 0.30Nb-doped BKT-BMT, the diffraction peaks shift to the lower diffraction angles because the ionic radius of Nb^{+5} (0.69 Å) is larger than that of Ti^{+4} (0.61 Å); as a result, the unit cell was expanded and the lattice parameter was increased with the replacement of Ti^{+4} by Nb^{+5} with Nb substitution.[19,20] Figure 3b shows the density of Nb-doped BKT-BMT ceramics at a sintering temperature of 1060°C and soaking time of 5 h. The unmodified ceramic sample had a density of 5.64 g/cm^3 (90% densification), while the 2-mol.%-Nb-modified sample showed an increased density value of 6.2 g/cm^3 (96% densification).[11,17] At a higher doping level, the density of the materials decreased, which may be due to the potentially increased volatility of Bi and K with increasing soaking time, resulting in the formation of secondary phases, as can be seen from XRD analysis.

The dielectric constant (ε_r) and loss (tan δ) of a poled Nb-doped BKT-BMT system (x = 0.00, 0.010, 0.020, and 0.030) were measured under various frequencies (1 kHz, 10 kHz, 100 kHz, and 1000 kHz) from room temperature up to 400°C, as shown in Fig. 4. The frequency-dispersive dielectric permittivity shows relaxor-type behavior for all compositions over a relatively wide temperature range. The major peak at the maximum ε_r

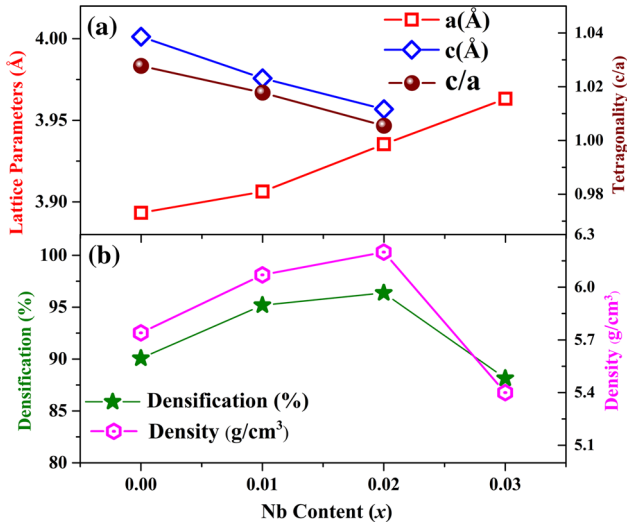

Fig. 3. (a) Lattice parameters *a*, *c* and tetragonality (*c*/*a*) of Nb-modified BKT-BMT ceramics (x = 0.00–0.030). (b) Density of Nb-modified BKT-BMT ceramics (x = 0.00, 0.010, 0.020, and 0.030) sintered at 1060°C.

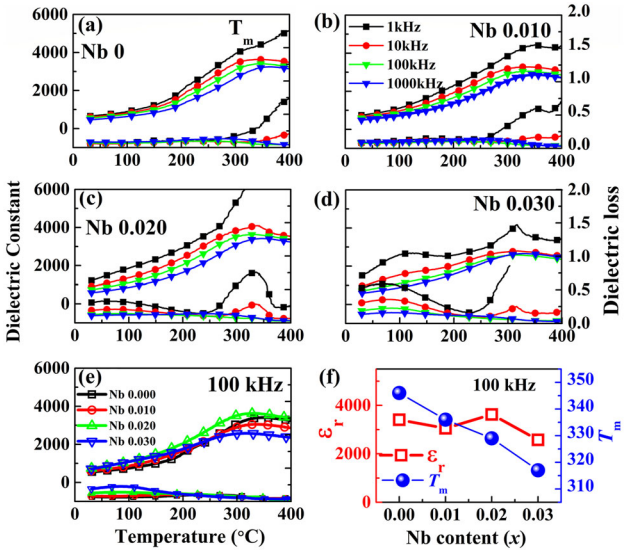

Fig. 4. Temperature dependence of dielectric constant and dielectric loss of poled Nb-modified BKT-BMT (x = 0.00, 0.010, 0.020, and 0.030) ceramics (a–d) as a function of different frequencies, (e) as a function of composition at 100 kHz, and (f) representative values of ε and T_m of as a function of composition.

temperature is referred to as the Curie temperature (T_m), as specified in dielectric curves and as shown in Fig. 4f. For all the investigated compositions, the broadening of the ε_r peak at T_m ($\sim$ 330°C) was observed, which can be attributed to the structural disordering, thermal randomization, and compositional fluctuations. This type of behavior has also been observed in other BKT-based systems.[12,18] For 0.03Nb, the tan δ decreases significantly at higher temperature above 200°C at 100 kHz, suggesting that the relatively low losses at high temperature compared to room temperature may arise from the short-range dielectric relaxation processes of polar nano-regions (PNRs) rather than the long-range conduction; similar behavior has also been observed in a BKT-$BiFeO_3$-$NdFeO_3$-$Nd_{2/3}TiO_3$ system.[14] The dielectric anomaly around 300°C can be attributed to the spontaneous transition between the high-temperature relaxor state and the low-temperature FE state. In the present system, the absence of a low-temperature dielectric anomaly depolarization temperature (T_d),[21–23] which is the main drawback of BNT-based materials, suggests that this system can work as a good FE material over a wide temperature range up to T_m. The absence of T_d at the low-temperature side of the dielectric permittivity, which was related to the irreversible phase transition from a nonergodic relaxor (NR) to FE state in the previous study of BNT-based systems,[19,20] also suggests the absence of the NR state in an Nb-doped BKT-BMT system. The possible reason for nonexistence of T_d at the low-temperature side of ε_r may be the shift of T_d toward the more dispersive higher-temperature region near T_m. In this high-temperature region, a spontaneous phase transition from thermalized ergodic relaxor (ER) state to a FE state may occur without any transition to the intermediate NR state.[2,16,19]

The FE hysteresis $P(E)$ loops for x = 0.00–0.030 were measured at room temperature (Fig. 5a). All the studied compositions with well-defined P–E loops without any contraction confirm the normal FE-like behavior of this system, which remain up to a high doping level. The FE properties of the base composition (x = 0.00) were effectively improved by Nb modification, as evidenced by an increase in remnant polarization P_r and a decrease in coercive field E_c, as shown in Fig. 5b. The P_r and E_c values change from $\sim$ 6 μC/cm^2 and $\sim$ 30 kV/cm for pure BKT-BMT to $\sim$ 13 μC/cm^2 and $\sim$ 22 kV/cm for x = 0.020, respectively. The maximum $P_r \sim$ 13 μC/cm^2 with $E_c \sim$ 22 kV/cm is comparable to the previous reports on BKT-based systems.[7,18] With further increase in Nb content, both P_r and E_c decrease. All the samples in the studied compositional range displayed normal FE-like behavior without apparent pinching and the corresponding NR-to-ER transition, which is in contrast with the BNT-based systems.[24–27] The piezoelectric sensor coefficient (d_{33}) improved from $\sim$ 53 pC/N for an unmodified sample to $\sim$ 68 pC/N for 2-mol.% Nb content, as seen from Fig. 6, which is in good agreement with FE properties. This increase in d_{33} at x = 0.020 may be ascribed to the onset of pseudocubic symmetry at the expense of tetragonal symmetry which then modified the multi-cationic bond lengths at a unit cell level and gave rise to more flexibility of complex domain switching.

The typical butterfly-shaped S–E loops with definite negative strain, shown in Fig. 7, further indicates the FE nature of the material and the

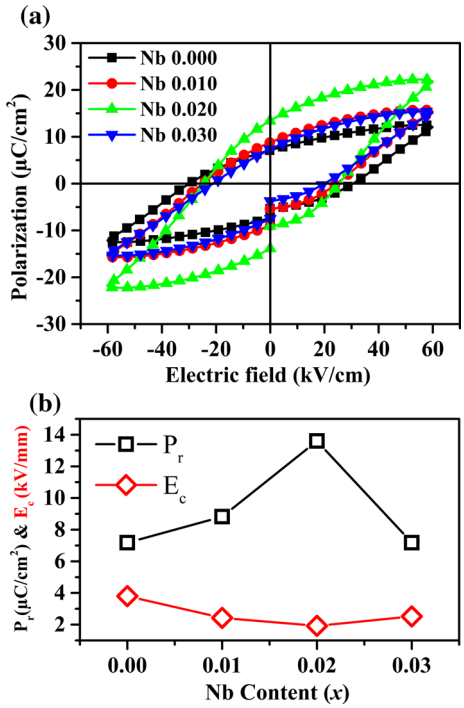

Fig. 5. (a) Effects of Nb substitution on the ferroelectric properties of BKT-BMT (x = 0.00–0.030) ceramics and (b) characteristics values of remnant polarization P_r and decrease in coercive field E_c.

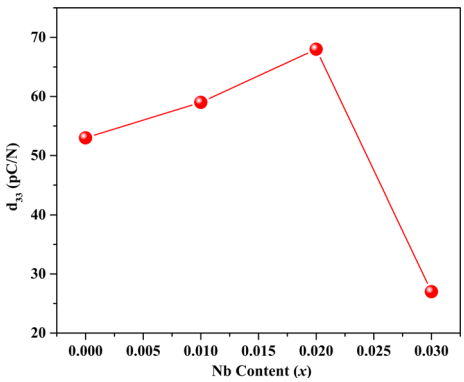

Fig. 6. Variation in piezoelectric constant (d_{33}) of Nb-modified BKT-BMT (x = 0.00–0.030) ceramics as a function of different compositions.

presence of an FE domain structure for all compositions. With increasing Nb content, the bipolar strain increases. Interestingly, both the positive strain and negative strain values increase with Nb concentration, in contrast with the BNT-based systems,[25,26] where the positive strain increases at the expense of negative strain. The sustainability and increase in negative strain confirm the presence of stable FE domains, and the progressive decrease in E_c indicates the easier domain back-switching under an external electric field. Furthermore, the material showed improved softening behavior with increasing Nb content, also clear form the P–E

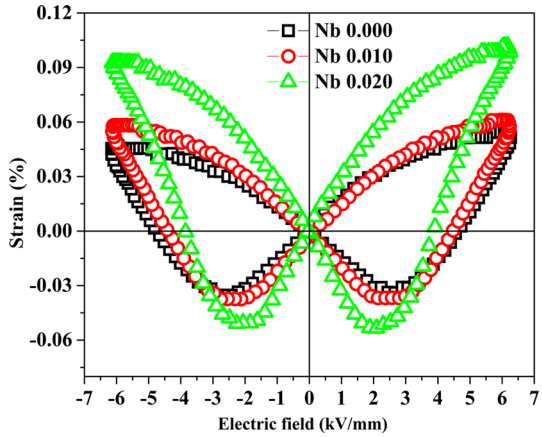

Fig. 7. The bipolar field-induced strain curves of the Nb-modified BKT-BMT ceramics.

loops. The hysteretic nature of P–E loops is also reflected in the S–E loops. The appearance of hysteresis for both P–E and S–E loops and high value of dielectric constant result from the spontaneous polarization from an ER state to an FE state, and confirm the presence of FE domains and their alignment with field direction which is one of the main sources of hysteresis loss in the material.

The observed strain of the present system is similar to typical FE materials, where the strain response is produced by two separate contributions, an intrinsic contribution due to the lattice distortion and an extrinsic contribution due to switching of FE domains and ever-present electrostriction. For BNT-based systems, the main contribution was from a near-nonpolar to a polar phase transition. Both the intrinsic and extrinsic responses lead to a change in the shape of FE materials due to application of an electric field. The intrinsic response results in the elongation and stretching of the unit cell due to the electric field, which is mainly related to a change in the magnitude of dipole moments and leads to an improved piezoelectric response for non-centrosymmetric materials, and the non-avoidable electrostriction for all types of materials. Meanwhile, the reorientation of FE domains contributes to the extrinsic strain response which may be the reorientation of dipole moments with constant magnitude (length).

The unipolar electric field-induced strain curves for Nb-doped BKT-BMT ceramics with x = 0.00, 0.010, and 0.020 are shown in Fig. 8. Similar to bipolar strain, the unipolar strain was increased significantly with increasing Nb content. At x = 0.020, field-induced strain of $S \sim 0.09\%$ and a corresponding normalized strain of $d^*_{33} \sim 140$ pm/V were observed. The large degree of hysteresis indicates that the high strain level is mainly derived from the combined effect of both extrinsic contribution originating from complex sluggish domain wall motion and intrinsic piezoelectric response ($d_{33} < 68$ pC/N) at the unit cell level. Similar strain

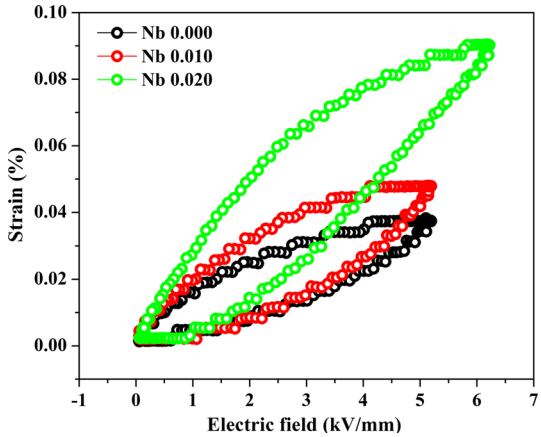

Fig. 8. Unipolar strain curves of Nb-modified BKT-BMT ceramics.

behavior had been observed in various Bi-based ceramics prepared by conventional solid-state reaction.[28–33]

In contrast to BNT-based ceramics where incorporation of small amounts of dopants strongly and abruptly affected the dielectric, FE, and field-induced strain properties, in the form of depolarization temperature, pinching of FE loops, and sudden increase in positive strain,[24–29] respectively, the BKT-based systems do not show such sharp anomalies. The main idea behind such abrupt changes in BNT-based materials was the formation of PNRs and their compositional-, temperature-, and field-assisted transition between their different dynamical states (ER and NR); the two well-known ER and NR states have been studied in literature thoroughly.[30–34] But, for the present BKT-based system, the absence of the depolarization anomaly (T_d) in the dielectric constant on the lower-temperature side for all samples, and the absence of a pinched P–E loop for the studied doping level, strongly support one of two possibilities: the absence of PNRs in the BKT system or the absence of an NR state in the BKT system. The first possibility seems to be not so reliable, because it is widely accepted that a relaxor state with the formation of PNRs is induced by local random fields resulting from randomly distributed different cations or lattice defects. Thus, the multi-occupancy of A- and B-site complex perovskite in BKT systems contradicts the first possibility and the formation of PNRs cannot be ceased.[35–37] Meanwhile, the second possibility relating to the nature of dynamical behavior of PNRs with the absence of NR to ER transition cannot be ignored. Thus, in BKT systems, freezing of PNRs appear at relatively high temperatures (at around T_m) which triggers the spontaneous ER-to-FE phase transition with the long-range FE order without any formation of an NR state at low temperature. Therefore, BKT-based materials show a normal FE-like behavior without any pinching at room temperature, while the BNT-based materials behave like NR at room temperature. Based on our results, it is proposed that Nb-doped BKT-BMT materials (unlike BNT-based materials) spontaneously transform from a high-temperature ER state to an FE state without any transition to an intermediate NR state.

CONCLUSION

Lead-free Nb-modified $0.96Bi_{0.5}K_{0.5}TiO_3$-$0.04Bi(Mg_{0.5}Ti_{0.5})O_3$ compositions were synthesized by a conventional solid-state reaction method. A pure perovskite phase with tetragonal symmetry was observed for undoped BKT-BMT compositions. The possible shift of depolarization temperature T_d toward high-temperature T_m may triggered the spontaneous relaxor-to-FE phase transition with an improved long-range FE order. The addition of Nb gradually decreases the tetragonality of BKT-BMT along with increase in d_{33} and P_r values. For $x = 0.020$, the structural phase transition from tetragonal to pseudocubic, with a maximum $d_{33} \sim 68$pC/N and highest FE response (~ 13 μC/cm^2), was observed at room temperature. This study suggests that the FE properties of the BKT system were significantly improved by Nb substitution. This enhancement can be linked to the flexibility of the tetragonal phase with Nb doping, which facilitates the development of the long-range order evident by an increase in $P_r \sim 13$ μC/cm^2 and negative strain values up to $x = 0.020$.

ACKNOWLEDGEMENT

This work was supported by the Basic Science Research Program through the National Research Foundation of Korea (NRF), as funded by the Ministry of Education, Science and Technology (MEST; 2011-0030058).

REFERENCES

1. J. Rödel, K.G. Webber, R. Dittmer, W. Jo, M. Kimura, and D. Damjanovic, *J. Eur. Ceram. Soc.* 35, 1659 (2015).
2. R.A. Malik, A. Hussain, A. Maqbool, A. Zaman, T.K. Song, W.J. Kim, and M.H. Kim, *J. Alloys Compd.* 682, 302 (2016).
3. C.H. Hong, H.P. Kim, B.Y. Choi, H.S. Han, J.S. Son, C.W. Ahn, and W. Jo, *J. Materiomics* 2, 1 (2016).
4. T. Rojac, A. Bencan, B. Malic, G. Tutuncu, J.L. Jones, J.E. Daniels, and D. Damjanovic, *J. Am. Ceram. Soc.* 97, 1993 (2014).
5. S.J. Zhang, R. Xia, and T.R. Shrout, *J. Electroceram.* 19, 251 (2007).
6. Y. Hiruma, R. Aoyagi, H. Nagata, and T. Takenaka, *Jpn. J. Appl. Phys.* 43, 7556 (2004).
7. Y. Hiruma, K. Yoshii, H. Nagata, and T. Takenaka, *J. Appl. Phys.* 103, 084121 (2008).
8. M.I. Morozov, M.A. Einarsrud, T. Grande, and D. Damjanovic, *Ferroelectrics* 439, 88 (2012).
9. H.L. Du, W.C. Zhou, F. Luo, D.M. Zhu, S.B. Qu, Y. Li, and Z.B. Pei, *J. Phys. D Appl. Phys.* 41, 115413 (2008).
10. M. Bengagi, F. Morini, M.E. Maaoui, and P. Marchet, *Phys. Status Solidi A* 209, 2063 (2012).
11. P. Jaita, P. Jarupoom, R. Yimnirun, G. Rujijanagul, and D.P. Cann, *Ceram. Int.* 42, 15940 (2016).
12. Z. Pan, Q. Wang, J. Chen, C. Liu, L. Fan, L. Liu, L. Fang, and X. Xing, *J. Am. Ceram. Soc.* 98, 104 (2015).
13. Y. Pu, P. Gao, T. Wu, X. Liu, and Z. Dong, *J. Electron. Mater.* 44, 332 (2015).

14. A. Khesro, D.W. Wang, F. Hussain, D.C. Sinclair, A. Feteira, and I.M. Reaney, *Appl. Phys. Lett.* 109, 142907 (2016).
15. A.J. Royles, A.J. Bell, A.P. Jephcoat, A.K. Kleppe, S.J. Milne, and T.P. Comyn, *Appl. Phys. Lett.* 97, 132909 (2010).
16. B. Hu, M. Zhu, J. Guo, Y. Wang, M. Zheng, and Y. Hou, *J. Am. Ceram. Soc.* 99, 1637 (2016).
17. A. Hussain, A. Maqbool, R.A. Malik, J.U. Rahman, T.K. Song, W.J. Kim, and M.H. Kim, *Ceram. Int.* 41, S26 (2015).
18. A. Zeb and S.J. Milne, *J. Am. Ceram. Soc.* 97, 2413 (2014).
19. A. Zaman, A. Hussain, R.A. Malik, A. Maqbool, S. Nahm, and M.H. Kim, *J. Phys. D Appl. Phys.* 49, 175301 (2016).
20. A. Maqbool, A. Hussain, R.A. Malik, J.U. Rahman, A. Zaman, T.K. Song, W.J. Kim, and M.H. Kim, *Mater. Sci. Eng., B* 199, 105 (2015).
21. H. Zhang, D. Zheng, S. Hu, C. Cheng, G. Peng, J. Zhang, and L.L. Li, *J. Mater. Sci.: Mater. Electron.* 28, 67 (2017).
22. V. Kalem, *J. Mater. Sci.: Mater. Electron.* 27, 8606 (2016).
23. A. Maqbool, A. Hussain, J.U. Rahman, J.K. Park, T.G. Park, J.S. Song, and M.H. Kim, *Phys. Status Solidi A* 211, 1709 (2014).
24. J. Yin, C. Zhao, Y. Zhang, and J. Wu, *J. Am. Ceram. Soc.* (2017). https://doi.org/10.1111/jace.15083.
25. L. Wu, B. Shen, Q. Hu, J. Chen, Y. Wang, Y. Xia, J. Yin, and Z. Liu, *J. Am. Ceram. Soc.* (2017). https://doi.org/10.1111/jace.15009.
26. R.A. Malik, A. Hussain, A. Zaman, A. Maqbool, J.U. Rahman, T.K. Song, W.J. Kim, and M.H. Kim, *RSC Adv.* 5, 96953 (2015).
27. A. Hussain, A. Maqbool, R.A. Malik, J.H. Lee, Y.S. Sung, T.K. Song, and M.H. Kim, *Ceram. Int.* 43, S204 (2017).
28. G. Dong, H. Fan, J. Shi, and M. Li, *J. Am. Ceram. Soc.* 98, 1150 (2015).
29. A. Ullah, C.W. Ahn, R.A. Malik, and I.W. Kim, *Phys. B* 444, 27 (2014).
30. R.F. Ge, Z.H. Zhao, S.F. Duan, X.Y. Kang, Y.K. Lv, D.S. Yin, and Y. Dai, *J. Alloys Compd.* 724, 1000 (2017).
31. X. Liu and X. Tan, *Adv. Mater.* 28, 574 (2016).
32. W. Bai, Y. Bian, J. Hao, B. Shen, and J. Zhai, *J. Am. Ceram. Soc.* 96, 246 (2013).
33. J. Hao, B. Shen, J. Zhai, C. Liu, X. Li, and X. Gao, *J. Appl. Phys.* 113, 114106 (2013).
34. R.A. Malik, A. Hussain, A. Maqbool, A. Zaman, C.W. Ahn, J.U. Rahman, T.K. Song, W.J. Kim, and M.H. Kim, *J. Am. Ceram. Soc.* 98, 3842 (2015).
35. S. Gao, Z. Yao, L. Ning, G. Dong, H. Fan, and Q. Li, *Adv. Eng. Mater.* (2017). https://doi.org/10.1002/adem.201700125.
36. H. Qi, R. Zuo, D. Zheng, and A. Xie, *J. Alloys Compd.* 724, 774 (2017).
37. X. Liu, J. Zhai, B. Shen, F. Li, and P. Li, *J. Electron. Mater.* 46, 5553 (2017).